

# Benchmarking DNA methylation assays in a reef-building coral

Groves Dixon  | Mikhail Matz

Department of Integrative Biology,  
University of Texas, Austin, TX, USA

## Correspondence

Groves Dixon, Department of Integrative  
Biology, University of Texas, Austin, TX,  
USA.  
Email: grovesdixon@gmail.com

## Funding information

NSF, Grant/Award Number: #1755277

## Abstract

Interrogation of chromatin modifications, such as DNA methylation, has the potential to improve forecasting and conservation of marine ecosystems. The standard method for assaying DNA methylation (whole genome bisulphite sequencing), however, is currently too costly to apply at the scales required for ecological research. Here, we evaluate different methods for measuring DNA methylation for ecological epigenetics. We compare whole genome bisulphite sequencing (WGBS) with methylated CpG binding domain sequencing (MBD-seq), and a modified version of MethylRAD we term methylation-dependent restriction site-associated DNA sequencing (mdRAD). We evaluate these three assays in measuring variation in methylation across the genome, between genotypes, and between polyp types in the reef-building coral *Acropora millepora*. We find that all three assays measure absolute methylation levels similarly for gene bodies (gbM), as well as exons and 1 Kb windows with a minimum Pearson correlation 0.66. Differential gbM estimates were less correlated, but still concurrent across assays. We conclude that MBD-seq and mdRAD are reliable and cost-effective alternatives to WGBS. The considerably lower sequencing effort required for mdRAD to produce comparable methylation estimates makes it particularly useful for ecological epigenetics.

## KEYWORDS

coral, DNA methylation, ecological epigenetics, gene body methylation, marine

## 1 | INTRODUCTION

The alarming effects of climate change on marine environments have led to a growing interest in Ecological Epigenetics. This relatively new field focused on the interrelationships between environment, epigenetic modification, gene expression, and phenotypic variation (Bossdorf et al., 2008), has the potential to improve forecasting and conservation of marine ecosystems. For instance, epigenetic modifications are hypothesized to mediate phenotypic plasticity, a mechanism important for resilience to environmental change (Eirin-Lopez & Putnam, 2019; Reusch, 2013). In humans, individuals prenatally exposed to famine show persistent differences in DNA methylation at relevant genes alongside alterations in disease risk (Heijmans et al., 2008; Painter et al., 2005). There is evidence that effects may extend even to the grandchildren of

those who experienced food shortage (Kaati et al., 2007). Evidence from other mammals adds further support for such intergenerational, and even transgenerational effects (Irlmer et al., 2020; Radford et al., 2014). In one remarkable case, traumatic olfactory conditioning in male mice was reported to produce epigenetic effects in F1s, and behavioural sensitivity even in F2s (Dias & Ressler, 2014). Intergenerational effects and maternal effects have also been reported in plants (Feil & Fraga, 2012), corals (Putnam & Gates, 2015; Liew et al., 2018; Liew et al., 2020), and sea urchins (Strader et al., 2019; Wong et al., 2018; Wong et al., 2018). While such reports are exciting, it is important to maintain a reserved view on the overall importance of epigenetics for adaptation, especially as many published examples await independent replication (Horsthemke, 2018) or have had attempts at replication fail to produce the same results (Irlmer et al., 2020).

A notable feature found in plants and invertebrates is an association between gene body methylation (methylation of CpG sites within coding regions; gbM), and gene expression. In both groups, genes with gbM tend to be actively and stably expressed, whereas those without gbM tend toward less active, inducible expression (Dimond & Roberts, 2016; Dixon et al., 2014, 2016; Gavery & Roberts, 2013; Sarda et al., 2012; Takuno & Gaut, 2012, 2013; Takuno et al., 2016; Zemach & Zilberman, 2010). Although gbM does not systematically regulate gene expression in plants or animals (Bewick et al., 2016, 2018, 2019; Choi et al., 2020; Harris et al., 2019; Zilberman, 2017), comparisons between populations may still be ecologically informative. Indeed, in the coral *Acropora millepora*, comparative methylomics predicted fitness characteristics of transplanted corals better than either SNPs or gene expression (Dixon et al., 2018). The potential to predict fitness in novel conditions is especially important for conservation efforts involving outplanting individuals to maintain and rescue wild populations (van Oppen et al., 2015, 2017). Hence there is a need for cost-effective examination of chromatin modifications in ecological contexts. While chromatin marks such as histone modifications are undoubtedly important (Eirin-Lopez & Putnam, 2019), DNA methylation is currently the easiest to measure, and the best-studied (Hofmann, 2017).

Here, we use a model reef-building coral, *Acropora millepora*, to benchmark methods for assaying DNA methylation. Reef-building corals are prime candidates for the application of ecological epigenetics. They are exceptional both in their socioecological value, and sensitivity to anthropogenic change (Cesar, 2000; Foden et al., 2013). Furthermore, as they are long-lived and sessile, they cannot migrate in response to suboptimal conditions, and must instead depend upon plasticity. Using this system, we compare three assays for measuring DNA methylation: Whole genome bisulphite sequencing (WGBS), methylated CpG binding domain sequencing (MBD-seq) (Serre et al., 2009), and a modified version of the MethylRAD (Wang et al., 2015). WGBS, considered the gold standard for measuring DNA methylation, works by chemical conversion of unmethylated cytosines to uracils. Following PCR amplification, these bases are read as thymines. Hence, when mapped against a reference, fold coverage of reads indicating cytosine at a given site relative to fold coverage indicating thymines quantifies the rate at which the site was methylated in the original DNA isolation. MBD-seq works by capturing methylated DNA fragments with methyl-CpG-binding domains affixed to magnetic beads. This methodology has been used previously for ecological studies in *A. millepora* (Dixon et al., 2016, 2018) and benchmarked against bisulphite sequencing in cultured embryonic stem cells (Harris et al., 2010). MethylRAD selects for methylated DNA through the activity of methylation-dependent restriction enzymes. DNA is digested with these enzymes, producing sticky ends exclusively near methylated recognition sites that allow for adapter ligation and sequencing. Methylation is quantified based on resulting fold coverage within a given region. The original MethylRAD protocol involved size selection for short fragments that were cut on both sides of palindromic methylated recognition

sequences (Wang et al., 2015). We have modified the protocol by size-selecting for all digestion-derived fragments in the 170–700 bp range. The method is now conceptually similar to the genotyping by sequencing (GBS) protocol described in Elshire et al. (2011) and Andrews et al. (2016). To differentiate it from the original methylRAD, we refer to it as methylation-dependent restriction site-associated DNA sequencing (mdRAD).

With these three assays, we examine variation in methylation between genomic regions, between two polyp types (axial and radial), and between coral colonies (genotypes). While they require less sequencing effort, and are less expensive to prepare on a per-sample basis, MBD-seq and mdRAD libraries do not provide quantitative, single-base resolution achievable with the gold standard WGBS. Hence MBD-seq and mdRAD represent a tradeoff of spatial and quantitative precision in exchange for larger sample sizes achievable at equivalent cost. To aid in the evaluation of these competing features, we compare results from each assay to assess how consistently they measure methylation, as well as the optimal sequencing effort to maximize sensitivity while minimizing costs.

## 2 | MATERIALS AND METHODS

### 2.1 | Sample collection

Two adult colonies of *A. millepora* were collected by SCUBA on 25 November 2018, one from Northeast Orpheus (labelled N12), and one from Little Pioneer Bay (labelled L5), under the Great Barrier Reef Marine Park Authority permit G18/41245.1. Colonies were maintained in the same raceway with flow of unfiltered seawater for 22 days. Branches from each colony were submerged in 100% ethanol and immediately placed at  $-80^{\circ}\text{C}$  for 48 hr. Samples were then maintained at  $-20^{\circ}\text{C}$  or on ice for approximately 48 hr during transport to the laboratory where they were again stored at  $-80^{\circ}\text{C}$  until processing.

### 2.2 | DNA Isolation

For each axial polyp sample, the very tips of four branches were cut off and pooled. For radial polyps, similar amounts of tissue were pooled from the sides of the same four branches. Tissue samples were lysed in Petri dishes with 2 ml of lysis buffer from an RNAqueous Total RNA Isolation Kit (Cat No. AM1912). DNA was isolated using phenol:chloroform:isoamyl alcohol with additional purification using a Zymo DNA cleanup and concentrator kit (Cat No. D4011) (Appendix S2). Isolations were quantified using a Quant-iT PicoGreen dsDNA Assay Kit (Cat No. P7589). The same DNA isolations were used for each downstream methylation assay. We isolated three replicates from each genotype-tissue pairing, for a total of 12 isolations (two colonies, two tissues, three replicates per). In downstream analyses, we use treatment groups to refer to either coral colony (N12 vs L5), or polyp type (tip vs side).

## 2.3 | Whole genome bisulphite sequencing library preparation

Whole genome bisulphite sequencing (WGBS) libraries were prepared using a Zymo Pico Methyl-Seq Library Prep Kit (Cat No. D5455). Each library was prepared from 100 ng of genomic DNA. For half the samples, we included 0.05 ng (0.05%) of  $\lambda$  phage standard DNA to estimate conversion efficiency. The final sample size was eight (two genotypes, two tissues, two replicates per; Table 1). The eight libraries were sequenced across four lanes on a HiSeq 2,500 for single-end 50 bp reads at The University of Texas Austin Genome Sequencing and Analysis Facility (GSAF). Single-end sequencing was recommended in the Zymo Pico Methyl-Seq manual.

## 2.4 | mdRAD library preparation

mdRAD libraries were prepared using a protocol based on Wang et al. (2015). Importantly, Wang et al. (2015) selected small sized fragments that had been cut on either end by the enzyme due to palindromic recognition sequences. In our hands, the yield of the palindrome-derived product was very low, so we instead sequenced any ligated fragments in the 170–700 bp range. We also used different oligonucleotide sequences, designed for similarity to those used in the current 2bRAD protocol (Table S1) (Dixon et al., 2015; Matz et al., 2018; [https://github.com/zoon/2bRAD\\_denovo](https://github.com/zoon/2bRAD_denovo)). A detailed version of the protocol used is included as Appendix S2. We prepared libraries using two different methylation-dependent endonucleases, FspE1 (NEB cat no. R0662S) and MspJ1 (NEB cat no. R0661S). For each library, we used 100 ng of genomic DNA as input. Digests were prepared with 0.4 units of endonuclease and the recommended amounts of enzyme activator solution and Cutsmart buffer (final volume = 15.0  $\mu$ l) and incubated at 37°C for 4 hr. We then heated the digests for 20 min to deactivate the enzymes (at 80°C for FspE1 and 65°C for MspJ1). All ligations were prepared with 0.2  $\mu$ M mdRAD 5ILL adapter, 0.2  $\mu$ M of the mdRAD 3ILLBC1 adapter, 800 units of T4 ligase, 1mM ATP (included in ligase buffer), and 10  $\mu$ l of digested DNA (final volume = 20  $\mu$ l). Ligations were incubated at 4°C overnight (approximately 12 hr). Ligase was then heat-inactivated by incubation at 65°C for 30 min.

Sequencing adapters and multiplex barcodes were then appended by PCR. Each PCR was prepared with 0.3 mM each dNTP, 0.15  $\mu$ M of the appropriate ILL\_Un primer, 0.15  $\mu$ M of the appropriate ILL\_BC primer, 0.2  $\mu$ M of the p5 primer, 0.2  $\mu$ M of the p7 primer, 1x Titanium taq buffer, 1x Titanium taq polymerase, and 7  $\mu$ l of ligation (final volume = 20  $\mu$ l) (Table S1). At this point in the protocol, all samples were distinguishable by the dual barcoding scheme. The concentration of each PCR product was quantified using PicoGreen dsDNA Assay Kit (Cat No. P7589). Based on these concentrations, 200 ng of each product was combined into a final pool with approximate concentration of 32 ng/ $\mu$ l. A portion of this pool was then size selected for 170–700 bp fragments using 2% agarose gel and purified using a QIAquick gel Extraction kit (Cat No. 28,704). After gel purification, the pool was sequenced with a single run on a NextSeq 500 for paired-end 75 bp reads at the University of Texas Genome Sequencing and Analysis Facility. The final number of libraries included in the pool was 24 (two genotypes, two tissues, two different restriction endonucleases, three replicates per combination; Table 1). As this methylation assay depends on fold coverage to infer methylation levels, single-end reads are a more cost-effective approach. We opted for paired-end reads in this case only to ensure proper product structure for benchmarking purposes.

## 2.5 | MBD-seq library preparation

MBD-seq libraries were prepared using a Diagenode MethylCap kit (Cat No. C02020010) as described previously (Dixon et al., 2016, 2018). Briefly, genomic DNA was sheared to a target size of 300–500 bp. Concentrations based on PicoGreen dsDNA assay on genomic DNA were assumed not to have changed during shearing. Because limited genomic DNA remained, we prepared these libraries from pools of genomic DNA for each genotype-tissue pair. Also due to limited genomic DNA, the two libraries for N12 tips were prepared using only 0.565  $\mu$ g as input. For the remaining libraries, half were prepared with 1  $\mu$ g of input and the other half from 1.5  $\mu$ g. During capture of methylated DNA, we retained the flow-through for sequencing, which we refer to as the unbound fraction. Captured methylated fragments were eluted from capture beads in one single total elution using high elution buffer. The final sample size was

**TABLE 1** Sample and library information

Assay	Treatment groups	Replicates	Samples	Library types	Total libraries	Raw reads	Final aligned reads
WGBS <sup>a</sup>	4	2	8	1	8	9.54E + 08	3.73E + 08
MBD-seq <sup>b</sup>	4	2	8	2 <sup>c</sup>	16	4.88E + 08	3.94E + 08
mdRAD	4	3	12	2 <sup>d</sup>	24	2.85E + 08	1.23E + 08

<sup>a</sup>Zymo Picomethyl Kit.

<sup>b</sup>Diagenode Methylcap Kit.

<sup>c</sup>Both captured and unbound fractions were sequenced.

<sup>d</sup>Separate libraries prepared with FspE1 and MspJ1.

eight (two genotypes, two tissues, two replicates per; Table 1). After capture, fragment size was assessed using 1.5% agarose gels. The captured and unbound fractions both ranged between 200 and 1,000 bp. These fragments were submitted to the University of Texas Genome Sequencing and Analysis Facility. Here the fragments were further sheared to a target size of 400 bp. This additional shearing was done to ensure appropriate library sizes of 300–500 bp for sequencing. Libraries were prepared with a NEBNext Ultra II DNA Library Preparation Kit (Cat No. E7645). Libraries were sequenced with a single run on a NextSeq 500 for single-end 75 bp reads.

## 2.6 | Whole genome bisulphite sequencing data processing

Raw reads were trimmed and quality filtered using cutadapt, simultaneously trimming low-quality bases from the 3' end (-q 20) and removing reads below 30 bp in length (-m 30) (Martin, 2011). Trimmed reads were mapped to the *A. millepora* reference genome (Fuller et al., 2020) using Bismark v0.17.0 (Krueger & Andrews, 2011) with adjusted mapping parameters (--score\_min L,0,-0.6) in --non-directional mode as indicated in the Pico Methyl-Seq Library Prep Kit manual. Methylation levels were extracted from the alignments using bismark\_methylation\_extractor with the --merge\_non\_CpG, --comprehensive, and --cytosine\_report arguments. At this point, CpG sites within the lambda DNA chromosome and the mitochondrial chromosome were set aside to assess conversion efficiency. Conversion efficiencies were estimated as the ratio of “unmethylated” fold coverage (converted by bisulphite treatment) to all fold coverage summed across CpG sites in the lambda DNA and the host mitochondrial reference sequences. Detailed steps used to process the WGBS reads are available on the git repository ([https://github.com/Groves-Dixon-Matz-laboratory/benchmarking\\_coral\\_methylation](https://github.com/Groves-Dixon-Matz-laboratory/benchmarking_coral_methylation)).

## 2.7 | MBD-seq data processing

Raw reads were trimmed and quality filtered using cutadapt simultaneously trimming low-quality bases from the 3' end (-q 20) and removing reads below 30 bp in length (-m 30) (Martin, 2011). Trimmed reads were mapped to the *A. millepora* reference genome (Fuller et al., 2020) with bowtie2 using the --local argument (Langmead & Salzberg, 2012). Alignments were sorted and indexed using samtools (Li et al., 2009), and PCR duplicates were removed using MarkDuplicates from Picard Toolkit (Broad Institute, 2019). Fold coverage for different regions (e.g., gene boundaries, exon boundaries, 1 Kb windows, etc.) was counted using multicov from BEDTools (Quinlan & Hall, 2010). Detailed steps used to process the MBD-seq reads are available on the git repository ([https://github.com/Groves-Dixon-Matz-laboratory/benchmarking\\_coral\\_methylation](https://github.com/Groves-Dixon-Matz-laboratory/benchmarking_coral_methylation)).

## 2.8 | mdRAD data processing

All mdRAD reads were expected to contain NNRWCC as the first six bases of the forward read, and ACAC as the first four bases of the reverse read (Table S1). The degenerate NNRW sequence in the forward read allows for discrimination of PCR duplicates, as uniquely ligated digestion products are unlikely (1/64) to bear identical sequences for these four bases. With this in mind, we used a custom python script to filter out any reads for which the first 20 bp was duplicated in a previous read (i.e., a likely PCR duplicate). At the same time, all paired end reads were filtered to retain only those with the expected NNRWCC beginning to the forward read and ACAC in the reverse read. These nontemplate bases were trimmed, along with adapters and low-quality bases using cutadapt (Martin, 2011). Trimmed reads were mapped to the *A. millepora* reference genome (Fuller et al., 2020) with bowtie2 using the --local argument (Langmead & Salzberg, 2012). Alignments were sorted and indexed using samtools (Li et al., 2009). Fold coverage for different region types was counted using multicov from BEDTools (Quinlan & Hall, 2010). Detailed steps used to process the mdRAD reads are available on the git repository ([https://github.com/Groves-Dixon-Matz-laboratory/benchmarking\\_coral\\_methylation](https://github.com/Groves-Dixon-Matz-laboratory/benchmarking_coral_methylation)).

## 2.9 | Designating of regions of interest

Statistical analyses for all three assays were based on windows recorded in bed files. These included genes, exons, upstream sequences, and tiled windows of varying sizes, as well as different types of repetitive elements. Region boundaries were identified from GFF files included with the *A. millepora* reference genome (Fuller et al., 2020). Intergenic and intronic regions were identified based on gene and exon boundaries using the BEDTools suite (Quinlan & Hall, 2010). Upstream sequences included 1 Kb upstream of each gene. These were intended to approximate promoter regions. Tiled windows were also generated using BEDTools. General statistics for these regions such as length, nucleotide content, and the number of CpGs, were extracted from the reference genome with a custom python script using SeqIO from Biopython (Cock et al., 2009). All downstream analyses of methylation level and differences between groups were based on these regions.

## 2.10 | Whole genome bisulphite statistical analysis

Statistical analyses of WGBS data were conducted on the .cov files output from Bismark. Analysis was conducted only on CpG sites. Methylation level was calculated in several ways. The simplest metric was the overall fractional methylation, calculated as the number of methylated counts divided by all counts summed across CpGs within the region.

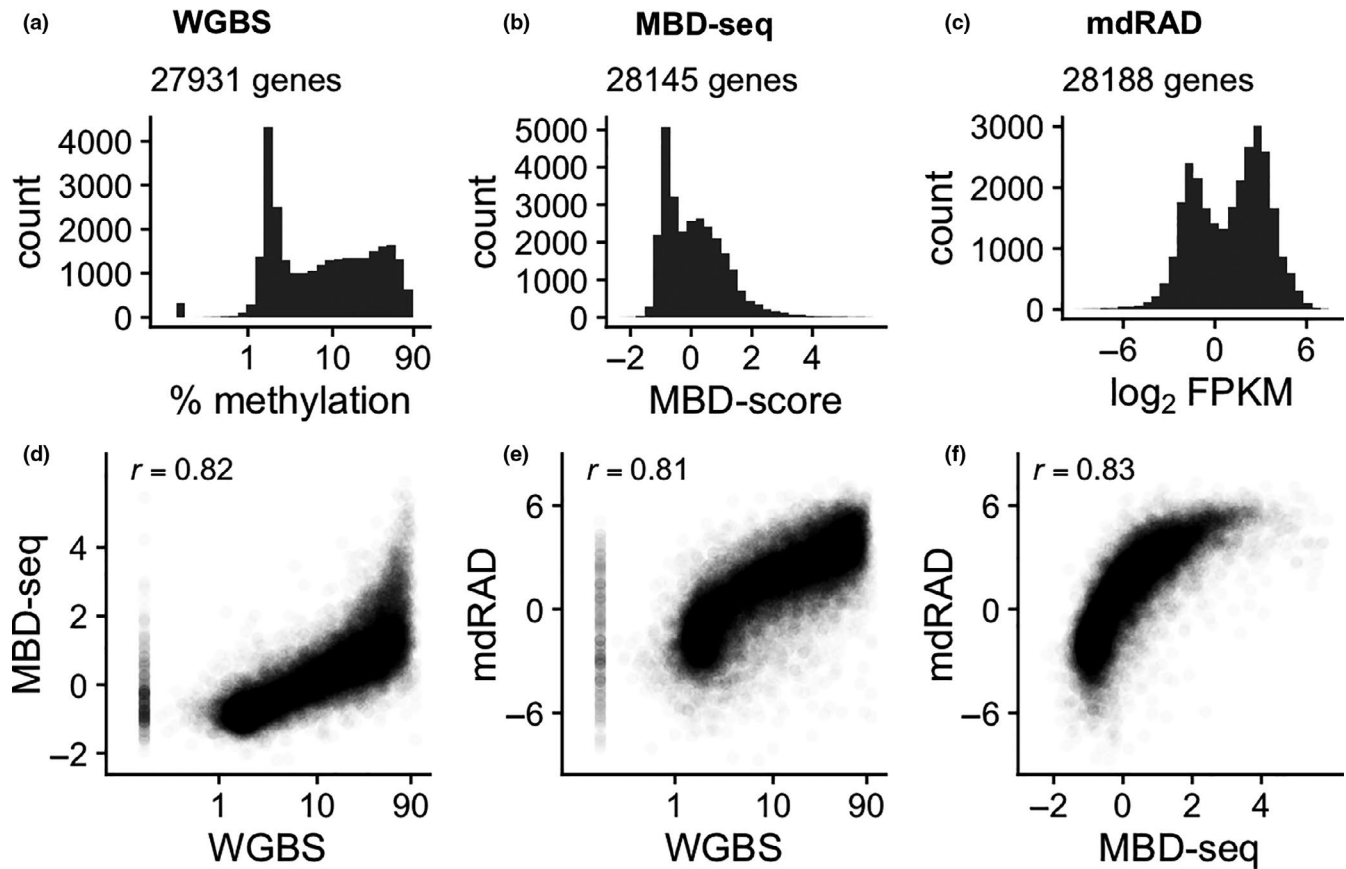


**FIGURE 1** Correlation of gbM level estimates from each assay. (a–c) Histograms of gbM level. (a) WGBS. Axis is on the  $\log_2$  scale. (b) MBD-seq. MBD-score refers to the  $\log_2$  fold difference between the captured (methylated) and unbound (unmethylated) fractions from the library preparation. (c) mdRAD. Plot shows  $\log_2$  FPKM from combined reads from both enzymes. (d–e) Scatterplots of methylation level estimates from each assay. Pearson correlations are indicated in the top left

We report this as the % methylation on the  $\log_2$  scale throughout the manuscript (e.g., Figure 1a). We calculated a similar metric using generalized logistic regression. Here the estimate of a region's methylation level was the sum of the intercept and the region's coefficient for a model of the probability of methylation given all methylated and unmethylated counts. We also report the frequency of methylated CpGs, calculated as the number of methylated CpG sites divided by the total number of CpG sites within a region. We classified a CpG as methylated when the number of methylated counts was significantly greater than the null expectation with 0.01 error rate (binomial test;  $p$ -value < .05). We also calculated the ratio of methylated CpGs to the total length (bp).

Statistical analysis of differences in methylation between treatment groups (tissue type or colony) was done with the MethylKit package (Akalin et al., 2012). Filtering parameters supplied to the filterByCoverage() function were lo.count = 5, and hi.perc = 99.9. The function methylKit::unite() was run using min.per.group = 4, so that only sites with data from all samples in each treatment group passed. Methylation counts for particular regions were isolated using the appropriate.bed file, the Granges() function from the GenomicRanges package (Lawrence et al., 2013), and the regionCounts() function from MethylKit.

## 2.11 | MBD-seq statistical analysis

Statistical analyses of MBD-seq data were conducted on the fold coverages output from BEDTools multicov. Methylation level was calculated based on the difference in fold coverage between the captured and unbound fractions taken during library preparation. We quantified this using DESeq2 as the  $\log_2$  fold change between the two fractions from a model including colony and polyp type as covariates (Love et al., 2014). Following previous studies (Dixon et al., 2016, 2018), we refer to this value as the MBD-score. We also calculated methylation level based on the fragments per kilobase per million reads (FPKM) from the captured fraction averaged across all samples. Differential methylation was also assessed using DESeq2. This was done in two ways, one using both the captured and unbound fractions, the other using only the captured fraction. Using both the captured and unbound fractions, the effect of treatment group was assessed as the interaction between treatment group and fraction. In other words, we assessed the effect of treatment group on the difference between the captured and unbound fractions. To assess methylation differences without using the unbound fraction, we modelled the counts from only the captured fraction using both treatment groups as predictors (polyp type and colony) then computed the contrasting  $\log_2$  fold changes for each

treatment group (tips vs sides and L5 vs N12). DESeq tests were run using `fitType = "local"` and significance was assessed using Wald tests.

## 2.12 | mdRAD statistical analysis

Statistical analyses of mdRAD data were conducted on the fold coverages output from BEDTools multicov. Methylation level was calculated as FPKM averaged across all samples, and as the fragments per recognition site per million reads. Methylation differences were calculated using DESeq2 comparing fold coverage between treatment groups while controlling for the restriction enzyme used and the other treatment group. DESeq tests were run using `fitType = "local"` and significance was assessed using Wald tests.

## 2.13 | Simulating reduced fold coverage

To assess the importance of fold coverage for methylation statistics, we simulated reduced fold coverages for each of the three assays. For MBD-seq and mdRAD, this was done by sampling genes with replacement weighted by the genes' proportion of total read counts in the original data set. This was done iteratively with increasingly lower sample sizes, simulating lower total counts. To clarify, to simulate read reductions for 28,188 genes for each sample, a vector of weights was generated by dividing each gene's fold coverage by the total for the sample. A vector of gene indices ranging from 1 to 28,188 was then randomly sampled with replacement, with probabilities set by the weight vector. The number of times each value was sampled was then totalled to give each genes' count in the simulated fold reduction. For WGBS, the trimmed fastq files were randomly sampled without replacement and all processing steps were repeated as indicated above.

## 2.14 | Gene ontology enrichment

Enrichment of gene ontology terms among genes not covered in the differential expression analysis was tested using Fisher's exact tests implemented using a custom R script (Wright et al., 2015; [https://github.com/z0on/GO\\_MWU](https://github.com/z0on/GO_MWU)).

## 2.15 | Statistical reporting

Unless otherwise noted, we report significant results as those with false discovery corrected *p*-values less than 0.1 (FDR < 0.1) (Benjamini & Hochberg, 1995). Correlations are reported as Pearson correlations. All scripts for data processing and analysis in this study are available on GitHub: ([https://github.com/Groves-Dixon-Matz-laboratory/benchmarking\\_coral\\_methylation](https://github.com/Groves-Dixon-Matz-laboratory/benchmarking_coral_methylation)).

## 3 | RESULTS

### 3.1 | WGBS sequencing results

Sequencing the WGBS libraries produced 954 million single-end reads across eight samples (two from each colony-tissue type pair; median = 120 million per sample). Trimming and quality filtering reduced the median to 119 million per sample. Mapping efficiency was 40% on average, with a median of 47 million mapped reads per sample (5.88x genomic coverage). Conversion efficiency averaged  $98.5 \pm \text{SE } 0.05\%$  based on spiked in lambda DNA and  $98.0 \pm \text{SE } 0.10\%$  based on mitochondrial DNA. The overall percentage of mapped reads was 39% of raw reads. The final fold coverage achieved for our WGBS libraries was below that recommended by the Zymo Pico Methyl-Seq Library Prep Kit Manual (D5455). Based on the cov files output by Bismark, mean per-sample CpG coverage ranged 5.16 to 6.22 (overall mean =  $5.58 \pm 0.001 \text{ SE}$ ). Hence, our WGBS results are based on very low coverage and should be considered largely for corroboration of the other two assays, rather than representative of the recommended WGBS methodology.

### 3.2 | MBD-seq sequencing results

Sequencing the MBD-seq libraries produced a total of 488 million single-end reads. These were divided across eight samples each with two libraries (one captured and one unbound). Median read count for the captured and unbound libraries was 27.4 and 33.1 million, respectively. Trimming and quality filtering removed 0.1% of reads. Mapping efficiency was 92% on average, with medians of 24.9 and 30.8 million reads for captured and unbound libraries respectively. PCR duplication rate was 12% on average, for final medians of 21.8 and 27.2 million mapped reads per sample for the captured and unbound fractions, respectively. The final percentage of countable reads (passing all filters and properly mapped) was 78% of raw reads for captured libraries and 82% for unbound libraries.

### 3.3 | mdRAD sequencing results

Sequencing the mdRAD libraries produced a total of 284 million paired-end reads across 24 libraries (three replicates for each of the four colony-polyp type combinations each prepared with two different restriction enzymes). These were filtered to include only reads with the appropriate adapter sequences found in both the forward and reverse directions (~71% of reads) and to remove PCR duplicates based on degenerate sequences incorporated into the forward read (average 13.5% duplication rate). On average 60% of raw reads passed both these filters (172 million total passing reads). Trimming and quality filtering further reduced this by 0.2%, for 74 million reads for Fspe1 libraries (median = 5.9 million per sample) and 98.5 million for the Mspj1 libraries (median = 7.3 million per sample). Properly paired mapping efficiency averaged 77% and 66%

for Fspe1 and Mspj1 libraries respectively, giving final median read counts of 4.6 and 4.9 million reads per library. The final percentage of raw reads that passed all filters and properly mapped was thus 44% for Fspe1 and 42% for MspJ1.

### 3.4 | Estimating methylation level

Measurements of absolute levels of gbM were consistent across assays. Each assay identified a bimodal distribution of gbM (Figure 1a–c). Pearson correlations between assays were all greater than 0.8 (Figure 1d–f). All three assays correlated negatively with the CpGo/e, with the strongest correlation found for WGBS (Figure S1). Correlations similar to those for gbM were found for exons (Figure S2), 1 Kb windows (Figure S3), and upstream regions of coding sequences (1 Kb upstream from the gene boundary) (Figure S4).

The measures of gbM level shown in Figure 1a–c were selected based on their simplicity and correlation between assays. Additional metrics of gbM level for WGBS, MBD-seq, and mdRAD are shown in Figures S5, S6 and S7. For WGBS, these included estimates based on logistic regression, the ratio of methylated CpGs to all CpGs, and the ratio of methylated CpGs to gene length. Of these, all except the

ratio of methylated CpGs to gene length correlated roughly equivalently with the other two assays (Figure S5). For MBD-seq, metrics that did not include the unbound fraction (FPKM and a similar metric based on the number of CpGs) correlated poorly with other assays (Figure S6). Hence sequencing the unbound fraction is important for measuring absolute methylation level with MBD-seq. For mdRAD, the two restriction enzymes produced nearly equivalent results. mdRAD FPKM was more consistent with other assays than a similar metric based on the number of recognition sites (Figure S7).

### 3.5 | Methylation differences between groups

Estimates of differential methylation between coral colonies were concordant between assays, but considerably less so than methylation level. Each assay identified extensive differential methylation between the two colonies (Figure 2a–c). The number of significant differentially methylated genes (DMGs) detected with each assay reflected the sample sizes used, rather than overall sequencing effort (Table 1). mdRAD, with 24 libraries, identified the most, with 12,244 DMGs. MBD-seq, with eight pairs of captured and flow-through libraries, identified the second most (7,268 DMGs). WGBS, with eight

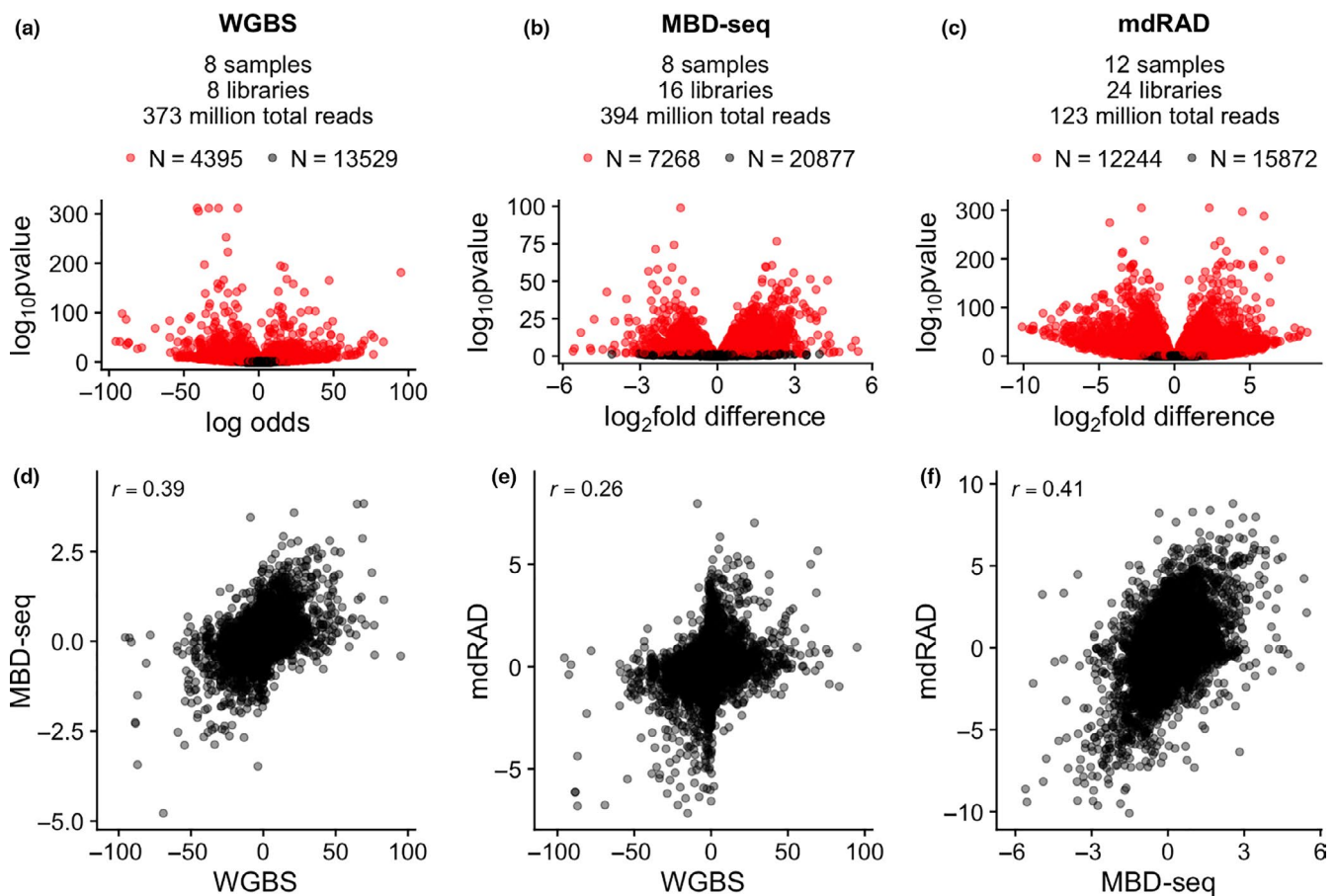


**FIGURE 2** Correlation of gbM difference estimates between two coral colonies (genotypes). (a–c) Volcano plots illustrating differential gbM for the indicated assay. Red points indicate significant genes (FDR < 0.1). The number of biological samples, libraries, total number of filtered and aligned reads, and the number of significant and nonsignificant genes is given in the subtitle for each panel. (d–f) Scatterplots of gbM difference estimates for the indicated assays. Pearson correlations are indicated in the top left [Colour figure can be viewed at [wileyonlinelibrary.com](http://wileyonlinelibrary.com)]

libraries, detected 4,395 DMGs. The overlap between these sets of DMGs is shown in Figure 3. Although it only used approximately 1/10th of the sequencing effort, a reduced mdRAD data set using only eight libraries generated with FspE1 still identified 7,407 DMGs (Figure S8).

Despite variations between assays and statistical methods, estimates of methylation differences were positively correlated (Figure 2d–f). MBD-seq correlated with the other two assays similarly (Pearson correlation = 0.39 and 0.41). mdRAD and WGBS were weakly correlated (Pearson correlation = 0.26). Correlations were stronger (0.31–0.55) when only methylated genes (> 3.1% methylation based on WGBS) were considered. Similar results were found for differences between exons (Figure S9), 1 Kb windows (Figure S10), and upstream regions of coding sequences (Figure S11). Hence, estimates of methylation differences between colonies (genotypes) were noisy, but reproducible across assays.

In contrast to differential methylation between colonies, differences between polyp types were weak, and not reproducible across assays. The number of significant differences was reversed compared to the colony comparison, with the most (169 DMGs) detected by WGBS, the second (12 DMGs) by MBD-seq, and the least (1 DMG) by mdRAD (Figure S12). There was no overlap in significant calls between assays. Difference estimates based on WGBS showed no correlation with the other two assays (Pearson correlation between 0.01 and 0.02). MBD-seq and mdRAD correlated weakly 0.2 (Figure S12).

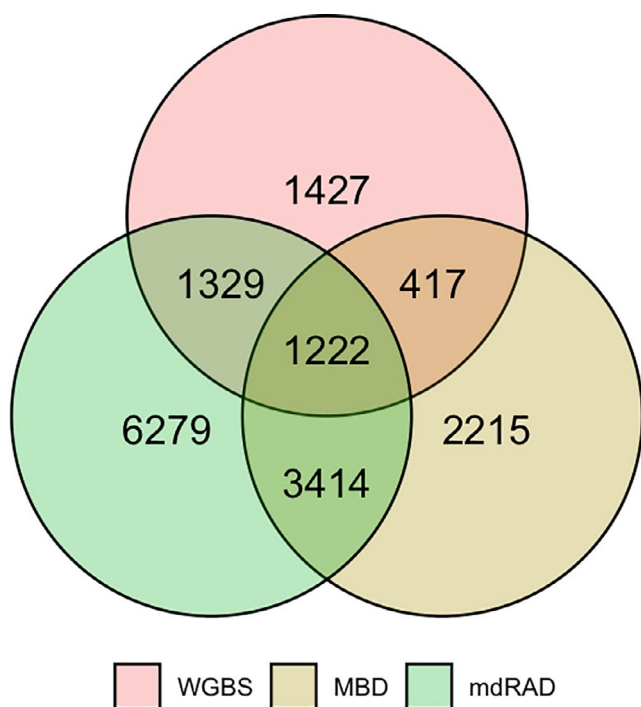


**FIGURE 3** Venn diagram showing overlap of differentially methylated genes detected with each assay. Overlap in significant genes was statistically significant for each pair (Fisher's exact test;  $p < 1 \times 10^{-6}$ ) [Colour figure can be viewed at [wileyonlinelibrary.com](http://wileyonlinelibrary.com)]

The methods also varied in their coverage for differential gbM (the number of genes for which differences were estimated). This is due to differences in sequencing effort and filtering parameters for each assay, and it should be noted that our WGBS libraries were shallowly sequenced (see Methods). The types of genes that were filtered from the WGBS differential methylation analysis were non-random with regard to gene function. Enriched GO terms for genes not covered by our WGBS data set are shown in (Figure S13). These included numerous terms for biological processes associated with immune response. No GO terms were significant for genes missing from the MBD-seq or mdRAD data sets.

### 3.6 | Spatial precision

Correlations between assays were generally robust across window sizes. For each assay, we calculated methylation level, as well as methylation differences between the two colonies for tiled windows of varying sizes: (100 bp, 500 bp, 1 Kb, 5 Kb, and 10 Kb). Correlations between assays were generally consistent across window sizes, both for methylation level and methylation differences (Figure 4). As with gbM, correlations for methylation level were much stronger (2–4-fold) than those for methylation differences. Hence, for the coral genome, MBD-seq and mdRAD reproducibly agree with the single-nucleotide measures from WGBS even across small regions.

To further characterize the assays, we examined their methylation level estimates for additional genomic regions with varying function and length, including introns, 5' UTRs, 3' UTRs, and intergenic regions, as well as repetitive elements including long interspersed nuclear elements (LINE), short interspersed nuclear elements (SINE), long tandem repeats (LTR), rolling circle repeats (RC), low complexity repeats, and simple repeats. Estimates of methylation levels for repetitive elements indicated that like coding genes, they tended to comprise mixtures of methylated and unmethylated elements (Figure S14). LTR and RC repeats appeared to have particularly high rates of methylation. The correlation of methylation level estimates between assays was lower for repetitive elements than for gene bodies, with a maximum correlation of 0.69 between MBD-seq and WGBS for LTRs, and lowest of 0.44 between mdRAD and WGBS for RC repeats (Figure S15). To further illustrate differences in coverage between our data sets, the proportion of total annotated elements passing filters for each assay are shown in Figure S16.

### 3.7 | Effect of fold coverage on detecting methylation differences

Given the importance of reducing sequencing costs for ecological epigenetics, we sought to evaluate the importance of sequencing effort for each assay in estimating methylation statistics. To do this, we simulated reduced sequencing effort by randomly resampling fold coverage from the data sets. We then recalculated estimates of methylation level and methylation differences from the reduced

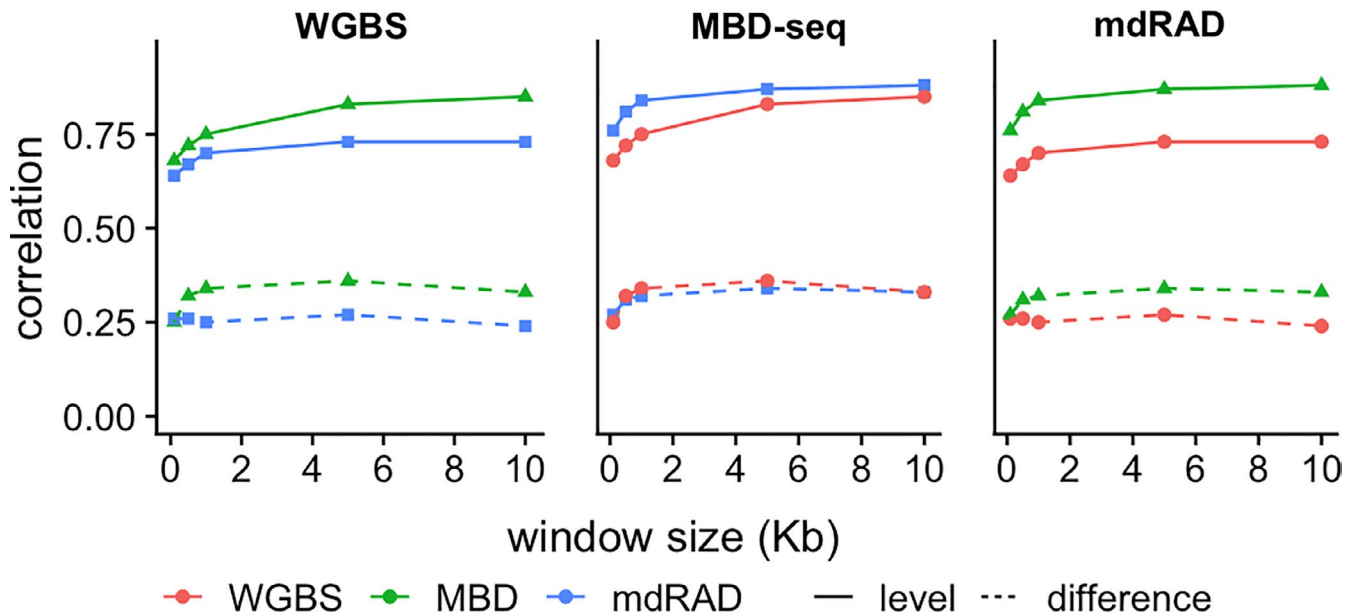


**FIGURE 4** Effect of window size on correlations between assays. Each panel indicates comparisons for one of the assays. Colours indicate the comparison assay. Solid lines indicate correlation of estimates of methylation level for the windows. Dotted lines indicate correlation for estimates of differential methylation between coral colonies [Colour figure can be viewed at [wileyonlinelibrary.com](http://wileyonlinelibrary.com)]

sets. As we detected no reproducible differences between polyp types (Figure S12), we focused on differences between colonies (genotype).

For estimates of absolute levels of gbM, fold coverage appeared to matter very little. We found that correlation between assays plateaued between 0.75 and 0.80 with approximately 20% of the original sequencing effort (Figure S17). Although lower, correlation of gbM differences also plateaued with relatively little sequencing effort (Figure 5a–c). Hence correlation between assays was sensitive only to severe reductions in fold coverage. Moreover, increasing fold coverage appeared unlikely to improve correlations between assays.

Detecting significant DMGs in contrast, was strongly dependent on fold coverage. For the sake of comparability, here we reduced the mdRAD data set to just eight libraries prepared with the FspE1 enzyme. To illustrate the importance of fold coverage for statistical significance, we made the simplifying assumption that a gene identified as differentially methylated by any two of the three assays was a “true” DMG. In other words, we assumed that the genes indicated by all overlapping regions of the Venn diagram shown in Figure 3 were “true” DMGs. We then plotted the proportion of these “true” DMGs that were also significant for a given read reduction (“any 2” trace in Figure 5d–f). This proportion provides an estimate of the assay's sensitivity at a given fold coverage. For a more stringent test of sensitivity, we also computed this value based on DMGs detected in each of the alternative assays (“alt. 2” in Figure 5d–f). For instance, for mdRAD, the DMGs for the alternative two assays are those identified as significant by both WGBS and MBD-seq. The “alt. 2” line, in this case, traces the proportion of this group of DMGs that was also significant for the indicated mdRAD fold coverage. Based on this analysis, it appeared that increasing sequencing effort would have returned many more DMGs for WGBS, somewhat more for

MBD-seq, and relatively few more for mdRAD. We also assessed how often DMG calls by each assay were corroborated by the other assays. Here we computed comparative precision as the proportion of DMGs from a given reduction that was also significant for at least two of the assays' full data sets (“any 2” in Figure 5g–i). For greater stringency, this was also computed based on significance in the two alternative assays (“alt 2” in Figure 5g–i). Corroboration rates were slightly higher for WGBS DMGs, but generally similar for all three assays. When we repeated the analysis using the full mdRAD data set (which still used less total sequencing; Table 1), mdRAD detected many more corroborated differences, with only slightly lower comparative precision (Figure S18). Costs for library preparation, and suggested targets for raw sequencing effort for each assay are included in Tables S2 and S3. In summary, mdRAD can identify reproducible differences in methylation with sensitivity and precision comparable to MBD-seq and a shallowly sequenced WGBS data set with relatively little fold coverage.

## 4 | DISCUSSION

Here, we present a benchmarking study of methods for assaying DNA methylation for ecological epigenetics in a marine invertebrate. We found that all three assays measure methylation level consistently, with a minimum correlation of 0.8 for gbM (Figure 1). Analysis of differential methylation was less consistent, but still indicated reproducible differences between coral colonies (Figure 2). Surprisingly, we found no such reproducible differences between polyp types (branch tips compared to branch sides; Figure S12). It is interesting to note that in this case, WGBS identified 169 DMGs, none of which were detected by the other assays. This may reflect

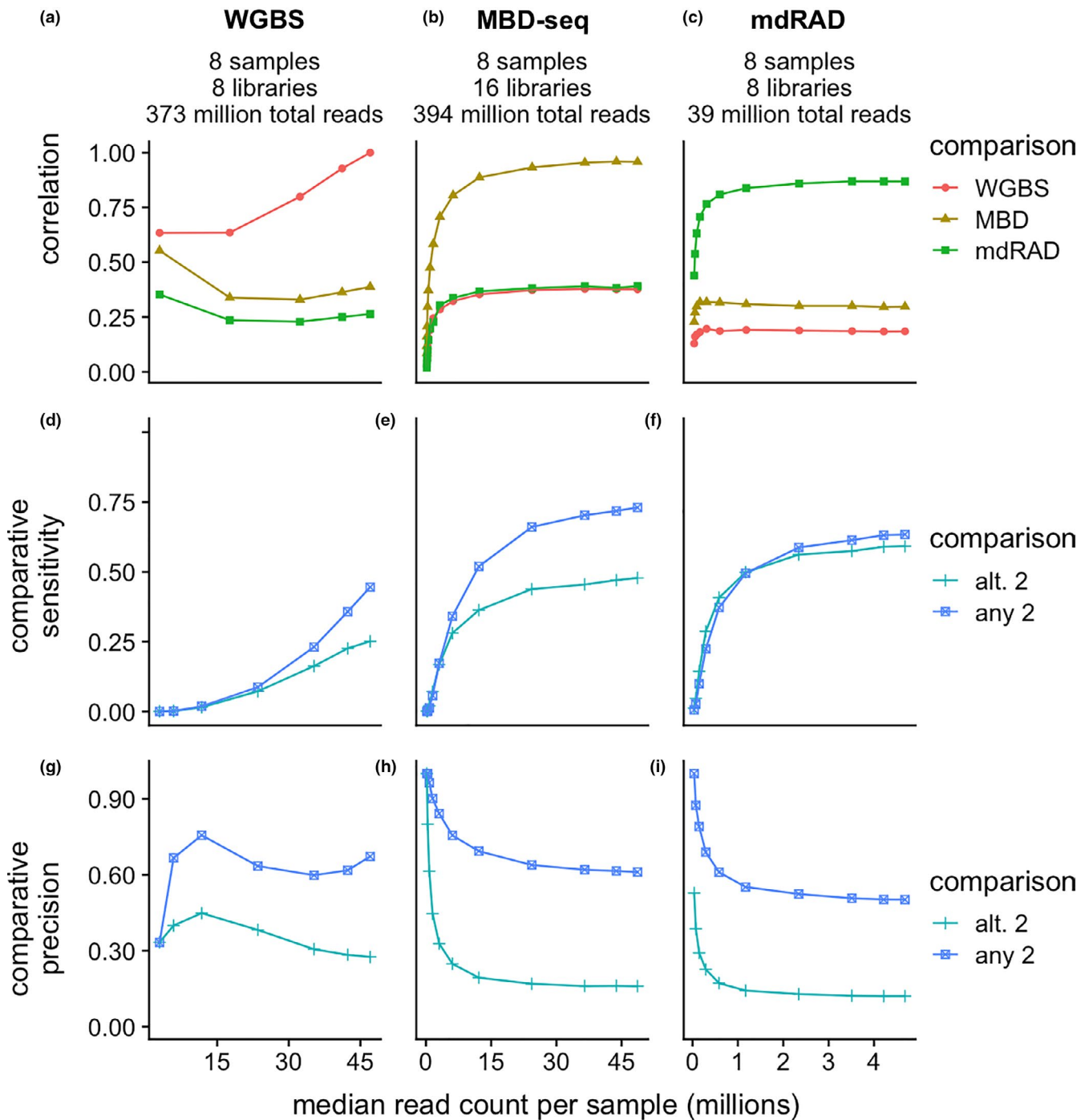


**FIGURE 5** Effect of simulated read reductions on estimates of methylation differences between coral colonies. Columns are assigned to the three assays. Rows are assigned to statistics measuring agreement between assays. Each data point represents a simulated reduction in fold coverage. (a–c) Pearson correlation between assays as fold coverage is reduced. (d–f) Sensitivity of each assay in detecting significant differences (FDR < 0.1) detected by other assays. For each reduction in fold coverage, comparative sensitivity is computed as the number of significant genes shared with the comparison divided by the total significant genes for the comparison. Comparisons include *any 2*: genes that were significant in any two assays; *alt. 2*: genes that were significant for both the alternative assays (g–i) Precision of each assay in detecting only significant differences (FDR < 0.1) also detected by other assays. For each reduction in fold coverage, comparative precision is computed as the number of significant genes shared with the comparison divided by the total significant genes for the fold reduction. Read counts on the X-axis refer to the total number of reads included in the final filtered alignment file, hence mapping efficiencies and PCR duplication rates should be accounted for when deciding on total sequencing effort [Colour figure can be viewed at [wileyonlinelibrary.com](http://wileyonlinelibrary.com)]

greater sensitivity of WGBS, even with the shallowly sequenced libraries used here. Indeed, a previous study applying WGBS with greater fold coverage detected substantial variation in methylation between oral and aboral tissue from the coral *Stylophora pistillata* (Liew et al., 2018). An alternative explanation is that there was little differential methylation between our polyp type samples, and the differences detected by our WGBS library were false positives.

Simulating reduced sequencing effort for each assay showed that fold coverage is most important in the context of statistical significance. While the number of corroborated DMGs dropped steeply with fold coverage (Figure 5d–f), correlations between assays were relatively stable (Figure 5a–c; Figure S18). This suggests that adding a second assay to a methylomic experiment can provide valuable corroboration even with relatively little sequencing effort. Based on these results, we suggest an experimental strategy that uses high fold coverage for one assay to obtain statistical significance and low coverage from another assay for corroboration. For instance, mdRAD could be used to sequence a large number of individuals to identify significant differences, with WGBS, MBD-seq, or both applied with relatively lower coverage for corroboration.

There are additional approaches for assessing DNA methylation that were not included in this study. For instance, reduced representation bisulphite sequencing (RRBS) is an approach for applying bisulphite sequencing to a subset of the genome (Gu et al., 2011). Briefly, genomic DNA is digested with a methylation insensitive restriction enzyme such as MspI, providing short fragments based on proximity to the enzyme's recognition site. Bisulphite conversion and sequencing of these fragments allows for quantitative, single-base resolution assessment of methylation levels. The selective process focuses sequencing effort on a subset of the genome, sacrificing the breadth of sites examined for greater fold coverage within the selected regions (Gu et al., 2011). A specific variant of RRBS is bsRADseq, which includes methodology for de novo analysis without a reference genome (Trucchi et al., 2016). As mdRAD also works through enzymatic selection, RRBS would probably provide comparable results regarding spatial precision (Figure 4), with the advantage of single-base resolution and quantitative measurement. Drawbacks to RRBS are increased complexity of library preparation and potentially decreased mapping efficiency (as observed with our WGBS data). Another option is MeDIP-seq, which uses antimethylcytosine antibodies to enrich for methylated DNA (Jacinto, Ballestar, & Esteller, 2008). This method is in principle very similar to MBD-seq, and the two methods have been shown previously to provide similar results (Harris et al., 2010). As calling SNPs from bisulphite data is problematic (Gao et al., 2015), the value of acquiring SNP data from the same set of NGS reads is also worth considering when selecting between bisulphite-based methods, such as RRBS and WGBS, and enrichment methods such as ME-DIP, MBD-seq and mdRAD.

The importance of spatial precision for a given study is another important consideration. In this study, we gave special attention to gbM, as it is the most common pattern of methylation described in invertebrates (Zemach & Zilberman, 2010). In some cases, this may reflect the spatial level at which variation in methylation patterns is

functionally relevant. For instance, evidence from plants indicates that methylation is evolutionarily conserved at the level of genes rather than individual sites (Takuno et al., 2016). Consistent with this hypothesis, Vidalis et al. (2016) found no evidence of selection at the level of single methylated sites. Alternatively, cases exist in mammalian systems where methylation status of single sites has functional importance (Nile et al., 2008; Zhang et al., 2010). Here, WGBS, or targeted bisulphite sequencing methods would be necessary. Hence an important consideration when selecting an assay is the genomic scale at which variation in methylation is expected to be ecologically relevant.

We have attempted to demonstrate the usefulness of both MBD-seq and mdRAD. These methods however, still represent a tradeoff of quantitative and spatial precision in exchange for reduced library preparation and sequencing costs. We have further suggested that an ideal strategy should include more than one methodology. To aid in evaluating these tradeoffs, we have included tables of the costs incurred for library preparation (Table S2) and suggested sequencing effort (Table S3) for each assay in this study. In evaluating the sequencing costs, we note that our WGBS libraries were undersequenced relative to the amount suggested in the Zymo Pico Methyl-Seq Library Prep Kit Manual (D5455) and as inferred from the sensitivity traces in Figure 5. While we cannot tell for certain how the number of significant genes detected would have changed with more WGBS sequencing effort, the steepness of the slopes in these curves is suggestive that more sequencing would have identified many more significant genes. We hope these data (Tables S2 and S3; and Figure 5) will be helpful in considering the tradeoffs between assays when developing an ecological methylation experiment.

To conclude, MBD-seq and mdRAD are cost-effective alternatives to WGBS. They provide consistent estimates of methylation level and are sensitive to methylation differences at relatively low library preparation and sequencing costs (Tables S2 and S3). The considerably lower sequencing effort required for mdRAD makes it particularly promising for the large sample sizes needed for ecological studies.

## ACKNOWLEDGEMENTS

This study was supported by the National Science Foundation grant IOS-1755277 to M.V.M. Data analysis was performed with the help of the Texas Advanced Computing Center.

## AUTHOR CONTRIBUTIONS

D.G. designed research, performed research, analysed data, and wrote the paper. M.M. designed the research and wrote the paper.

## DATA AVAILABILITY STATEMENT

Reads generated for this study have been uploaded to the SRA database project accession PRJNA601565. All scripts for data processing and analysis, as well as intermediate data sets are available on Github ([https://github.com/Groves-Dixon-Matz-laboratory/benchmarking\\_coral\\_methylation](https://github.com/Groves-Dixon-Matz-laboratory/benchmarking_coral_methylation)) (<https://doi.org/10.5281/zenodo.4012450>; Dixon, 2020). Bismark output files are also available

on Github ([https://github.com/groves-dixon-matz-laboratory/benchmarking\\_coral\\_methylation\\_data.git](https://github.com/groves-dixon-matz-laboratory/benchmarking_coral_methylation_data.git)) (<https://doi.org/10.5281/zenodo.4012456>).

## ORCID

Groves Dixon  <https://orcid.org/0000-0001-5501-6024>

## REFERENCES

- Akalin, A., Kormaksson, M., Li, S., Garrett-Bakelman, F. E., Figueroa, M. E., Melnick, A., & Mason, C. E. (2012). MethyKit: A comprehensive R package for the analysis of genome-wide DNA methylation profiles. *Genome Biology*, 13(10), <https://doi.org/10.1186/gb-2012-13-10-R87>
- Andrews, K. R., Good, J. M., Miller, M. R., Luikart, G., & Hohenlohe, P. A. (2016). Harnessing the power of RADseq for ecological and evolutionary genomics. *Nature Reviews Genetics*, 17, 81–92. <https://doi.org/10.1038/nrg.2015.28>
- Benjamini, Y., & Hochberg, Y. (1995). Controlling the false discovery rate: a practical and powerful approach to multiple testing. *Journal of the Royal Statistical Society*, 57(1), 289–300.
- Bewick, A. J., Ji, L., Niederhuth, C. E., Willing, E.-M., Hofmeister, B. T., Shi, X., Wang, L. I., Lu, Z., Rohr, N. A., Hartwig, B., Kiefer, C., Deal, R. B., Schmutz, J., Grimwood, J., Stroud, H., Jacobsen, S. E., Schneeberger, K., Zhang, X., & Schmitz, R. J. (2016). On the origin and evolutionary consequences of gene body DNA methylation. *Proceedings of the National Academy of Sciences of the United States of America*, 113(32), 9111–9116. <https://doi.org/10.1073/pnas.1604666113>
- Bewick, A. J., Sanchez, Z., McKinney, E. C., Moore, A. J., Moore, P. J., & Schmitz, R. J. (2018). Gene-regulatory independent functions for insect DNA methylation. *BioRxiv Preprint*. 355669, 1–33. <https://doi.org/10.1101/355669>
- Bewick, A. J., Zhang, Y., Wendte, J. M., Zhang, X., & Schmitz, R. J. (2019). Evolutionary and Experimental Loss of Gene Body Methylation and Its Consequence to Gene Expression. *G3: Genes|genomes|genetics*, 9(8), 2441–2445. <https://doi.org/10.1534/g3.119.400365>
- Bosssdorf, O., Richards, C. L., & Pigliucci, M. (2008). Epigenetics for ecologists. *Ecology Letters*, 11(2), 106–115. <https://doi.org/10.1111/j.1461-0248.2007.01130.x>
- Broad Institute. (2019). *Picard Toolkit*. Broad Institute.
- Cesar, H. S. J. (2000). Coral reefs: Their functions, threats and economic value. In H. S. J. Cesar (Ed.), *Collected essays on the economics of coral reefs*, (14–39). CORDIO, Department for Biology and Environmental Sciences, Kalmar University.
- Choi, J., Lyons, D. B., Kim, M. Y., Moore, J. D., Choi, J., Lyons, D. B., & Zilberman, D. (2020). DNA methylation and histone H1 jointly repress transposable elements and aberrant intragenic DNA methylation and histone H1 jointly repress transposable elements and aberrant intragenic transcripts. *Molecular Cell*, 77(2), 310–323. <https://doi.org/10.1016/j.molcel.2019.10.011>
- Cock, P. J. A., Antao, T., Chang, J. T., Chapman, B. A., Cox, C. J., Dalke, A., Friedberg, I., Hamelryck, T., Kauff, F., Wilczynski, B., & de Hoon, M. J. L. (2009). Biopython: freely available python tools for computational molecular biology and bioinformatics. *Bioinformatics*, 25(11), 1422–1423. <https://doi.org/10.1093/bioinformatics/btp163>
- Dias, B. G., & Ressler, K. J. (2014). Parental olfactory experience influences behavior and neural structure in subsequent generations. *Nature Neuroscience*, 17(1), 89–96. <https://doi.org/10.1038/nn.3594>
- Dimond, J. L., & Roberts, S. B. (2016). Germline DNA methylation in reef corals: Patterns and potential roles in response to environmental change. *Molecular Ecology*, 25, 1895–1904. <https://doi.org/10.1111/mec.13414>
- Dixon, G. (2020). Data from: benchmarking coral methylation git repository. PRJNA601565
- Dixon, G., Bay, L. K., & Matz, M. V. (2014). Bimodal signatures of germline methylation are linked with gene expression plasticity in the coral *Acropora millepora*. *BMC Genomics*, 15, 1109. <https://doi.org/10.1186/1471-2164-15-1109>
- Dixon, G., Bay, L. K., & Matz, M. V. (2016). Evolutionary consequences of DNA methylation in a basal metazoan. *Molecular Biology and Evolution*, 33(9), 2285–2293. <https://doi.org/10.1101/043026>
- Dixon, G. B., Davies, S. W., Aglyamova, G. V., Meyer, E., Bay, L. K., & Matz, M. V. (2015). Genomic determinants of coral heat tolerance across latitudes. *Science*, 348(6242), 1460–1462.
- Dixon, G., Liao, Y., Bay, L. K., & Matz, M. V. (2018). Role of gene body methylation in acclimatization and adaptation in a basal metazoan. *Proceedings of the National Academy of Sciences of the United States of America*, 115(52), 13342–13346. <https://doi.org/10.1073/pnas.1813749115>
- Eirin-Lopez, J. M., & Putnam, H. M. (2019). Marine environmental epigenetics. *Annual Review of Marine Science*, 11(1), 335–368. <https://doi.org/10.1146/annurev-marine-010318-095114>
- Elshire, R. J., Glaubitz, J. C., Sun, Q., Poland, J. A., Kawamoto, K., Buckler, E. S., & Mitchell, S. E. (2011). A robust, simple genotyping-by-sequencing (GBS) approach for high diversity species. *PLoS One*, 6(5), 1–10. <https://doi.org/10.1371/journal.pone.0019379>
- Feil, R., & Fraga, M. F. (2012). Epigenetics and the environment: Emerging patterns and implications. *Nature Reviews. Genetics*, 13(2), 97–109. <https://doi.org/10.1038/nrg3142>
- Foden, W. B., Butchart, S. H. M., Stuart, S. N., Vié, J.-C., Akçakaya, H. R., Angulo, A., DeVantier, L. M., Gutsche, A., Turak, E., Cao, L., Donner, S. D., Katariya, V., Bernard, R., Holland, R. A., Hughes, A. F., O'Hanlon, S. E., Garnett, S. T., Şekercioğlu, Ç. H., & Mace, G. M. (2013). Identifying the world's most climate change vulnerable species: A systematic trait-based assessment of all birds, amphibians and corals. *PLoS One*, 8(6), e65427. <https://doi.org/10.1371/journal.pone.0065427>
- Fuller, Z. L., Mocellin, V. J. L., Morris, L. A., Cantin, N., Shepherd, J., Sarre, L., & Przeworski, M. (2020). Population genetics of the coral *Acropora millepora*: Toward genomic prediction of bleaching. *Science (New York, N.Y.)*, 369(eaba4674), 1–9. <https://doi.org/10.1126/science.aba4674>
- Gao, S., Zou, D., Mao, L., Liu, H., Song, P., Chen, Y., ... Bolund, L. (2015). BS-SNPer: SNP calling in bisulfite-seq data. *Bioinformatics*, 31(24), 4006–4008. <https://doi.org/10.1093/bioinformatics/btv507>
- Gavery, M. R., & Roberts, S. B. (2013). Predominant intragenic methylation is associated with gene expression characteristics in a bivalve mollusc. *PeerJ*, 1, e215. <https://doi.org/10.7717/peerj.215>
- Gu, H., Smith, Z. D., Bock, C., Boyle, P., Gnirke, A., & Meissner, A. (2011). Preparation of reduced representation bisulfite sequencing libraries for genome-scale DNA methylation profiling. *Nature Protocols*, 6(4), 468–481. <https://doi.org/10.1038/nprot.2010.190>
- Harris, K. D., Lloyd, J. P. B., Domb, K., Zilberman, D., & Zemach, A. (2019). DNA methylation is maintained with high fidelity in the honey bee germline and exhibits global non-functional fluctuations during somatic development. *Epigenetics and Chromatin*, 12(1), 1–18. <https://doi.org/10.1186/s13072-019-0307-4>
- Harris, R. A., Wang, T., Coarfa, C., Nagarajan, R. P., Hong, C., Downey, S. L., Johnson, B. E., Fouse, S. D., Delaney, A., Zhao, Y., Olshen, A., Ballinger, T., Zhou, X., Forsberg, K. J., Gu, J., Echipare, L., O'Geen, H., Lister, R., Pelizzola, M., ... Costello, J. F. (2010). Comparison of sequencing-based methods to profile DNA methylation and identification of monoallelic epigenetic modifications. *Nature Biotechnology*, 28(10), 1097–1105. <https://doi.org/10.1038/nbt.1682>
- Heijmans, B. T., Tobi, E. W., Stein, A. D., Putter, H., Blauw, G. J., Susser, E. S., Slagboom, P. E., & Lumey, L. H. (2008). Persistent epigenetic differences associated with prenatal exposure to famine in humans. *Proceedings of the National Academy of Sciences of the United*

- States of America*, 105(44), 17046–17049. <https://doi.org/10.1073/pnas.0806560105>
- Hofmann, G. E. (2017). Ecological Epigenetics in Marine Metazoans. *Frontiers in Marine Science*, 4(January), 1–7. <https://doi.org/10.3389/fmars.2017.00004>
- Horsthenke, B. (2018). A critical view on transgenerational epigenetic inheritance in humans. *Nature Communications*, 9(1), 1–4. <https://doi.org/10.1038/s41467-018-05445-5>
- Irmeler, M., Kaspar, D., Hrab, M., Angelis, D., & Beckers, J. (2020). The (not so) Controversial Role of DNA Methylation in Epigenetic Inheritance Across Generations ethylation of Cytosine Represses Gene Expression. In R. Teperino (Ed.), *Beyond our genes* (pp. 175–208). Springer.
- Jacinto, F. V., Ballestar, E., & Esteller, M. (2008). Methyl-DNA immunoprecipitation (MeDIP): Hunting down the DNA methylome. *BioTechniques*, 44(1), 35–43. <https://doi.org/10.2144/000112708>
- Kaati, G., Bygren, L. O., Pembrey, M., & Sjöström, M. (2007). Transgenerational response to nutrition, early life circumstances and longevity. *European Journal of Human Genetics*, 15(7), 784–790. <https://doi.org/10.1038/sj.ejhg.5201832>
- Krueger, F., & Andrews, S. R. (2011). Bismark: A flexible aligner and methylation caller for Bisulfite-Seq applications. *Bioinformatics*, 27(11), 1571–1572. <https://doi.org/10.1093/bioinformatics/btr167>
- Langmead, B., & Salzberg, S. L. (2012). Fast gapped-read alignment with Bowtie 2. *Nature Methods*, 9(4), 357–359. <https://doi.org/10.1038/nmeth.1923>
- Lawrence, M., Huber, W., Pagès, H., Aboyoun, P., Carlson, M., Gentleman, R., Morgan, M. T., & Carey, V. J. (2013). Software for Computing and Annotating Genomic Ranges. *PLOS Computational Biology*, 9(8), 1–10. <https://doi.org/10.1371/journal.pcbi.1003118>
- Li, H., Handsaker, B., Wysoker, A., Fennell, T., Ruan, J., Homer, N., Marth, G., Abecasis, G., & Durbin, R. (2009). The Sequence Alignment/Map format and SAMtools. *Bioinformatics*, 25(16), 2078–2079. <https://doi.org/10.1093/bioinformatics/btp352>
- Liew, Y. J., Howells, E. J., Wang, X., Michell, C. T., Burt, J. A., Idaghdour, Y., & Aranda, M. (2020). Intergenerational epigenetic inheritance in reef-building corals. *Nature Climate Change*, 10(3), 254–259. <https://doi.org/10.1038/s41558-019-0687-2>
- Liew, Y. J., Zoccola, D., Li, Y., Tambutté, E., Venn, A. A., Michell, C. T., ... Aranda, M. (2018). Epigenome-associated phenotypic acclimatization to ocean acidification in a reef-building coral. *Science Advances*, 4, eaar8028. <https://doi.org/10.1101/188227>
- Love, M. I., Huber, W., & Anders, S. (2014). Moderated estimation of fold change and dispersion for RNA-Seq data with DESeq2. *Genome Biology*, 15(550), 1–21. <https://doi.org/10.1101/002832>
- Martin, M. (2011). Cutadapt removes adapter sequences from high-throughput sequencing reads. *EMBnet journal*, 17(1), 10–12. <https://doi.org/10.14806/ej.17.1.200>
- Matz, M. V., Tremblay, E. A., Aglyamova, G. V., & Bay, L. K. (2018). Potential and limits for rapid genetic adaptation to warming in a Great Barrier Reef coral. *PLOS Genetics*, 14(4), 1–19. <https://doi.org/10.1371/journal.pgen.1007220>
- Nile, C. J., Read, R. C., Akil, M., Duff, G. W., & Wilson, A. G. (2008). Methylation status of a single CpG site in the IL6 promoter is related to IL6 messenger RNA levels and rheumatoid arthritis. *Arthritis and Rheumatism*, 58(9), 2686–2693. <https://doi.org/10.1002/art.23758>
- Oppen, M. J. H., Gates, R. D., Blackall, L. L., Cantin, N., Chakravarti, L. J., Chan, W. Y., Cormick, C., Crean, A., Damjanovic, K., Epstein, H., Harrison, P. L., Jones, T. A., Miller, M., Pears, R. J., Peplow, L. M., Raftos, D. A., Schaffelke, B., Stewart, K., Torda, G., ... Putnam, H. M. (2017). Shifting paradigms in restoration of the world's coral reefs. *Global Change Biology*, 23(9), 3437–3448. <https://doi.org/10.1111/gcb.13647>
- Painter, R. C., Roseboom, T. J., & Bleker, O. P. (2005). Prenatal exposure to the Dutch famine and disease in later life: An overview. *Reproductive Toxicology*, 20, 345–352. <https://doi.org/10.1016/j.reprotox.2005.04.005>
- Putnam, H. M., & Gates, R. D. (2015). Preconditioning in the reef-building coral *Pocillopora damicornis* and the potential for trans-generational acclimatization in coral larvae under future climate change conditions. *Journal of Experimental Biology*, 218(15), 2365–2372. <https://doi.org/10.1242/jeb.123018>
- Quinlan, A. R., & Hall, I. M. (2010). BEDTools: A flexible suite of utilities for comparing genomic features. *Bioinformatics*, 26(6), 841–842. <https://doi.org/10.1093/bioinformatics/btq033>
- Radford, E. J., Ito, M., Shi, H., Corish, J. A., Yamazawa, K., Isganaitis, E., Seisenberger, S., Hore, T. A., Reik, W., Erkek, S., Peters, A. H. F. M., Patti, M.-E., & Ferguson-Smith, A. C. (2014). In utero undernourishment perturbs the adult sperm methylome and intergenerational metabolism. *Science*, 345(6198), <https://doi.org/10.1126/science.1255903>
- Reusch, T. B. H. (2013). Climate change in the oceans: Evolutionary versus phenotypically plastic responses of marine animals and plants. *Evolutionary Applications*, 7, 104–122. <https://doi.org/10.1111/eva.12109>
- Sarda, S., Zeng, J., Hunt, B. G., & Yi, S. V. (2012). The evolution of invertebrate gene body methylation. *Molecular Biology and Evolution*, 29(8), 1907–1916. <https://doi.org/10.1093/molbev/mss062>
- Serre, D., Lee, B. H., & Ting, A. H. (2009). MBD-isolated genome sequencing provides a high-throughput and comprehensive survey of DNA methylation in the human genome. *Nucleic Acids Research*, 38(2), 391–399. <https://doi.org/10.1093/nar/gkp992>
- Strader, M. E., Wong, J. M., Kozal, L. C., Leach, T. S., & Hofmann, G. E. (2019). Parental environments alter DNA methylation in offspring of the purple sea urchin, *Strongylocentrotus purpuratus*. *Journal of Experimental Marine Biology and Ecology*, 517(February), 54–64. <https://doi.org/10.1016/j.jembe.2019.03.002>
- Takuno, S., & Gaut, B. S. (2012). Body-methylated genes in *Arabidopsis thaliana* are functionally important and evolve slowly. *Molecular Biology and Evolution*, 29(1), 219–227. <https://doi.org/10.1093/molbev/msr188>
- Takuno, S., & Gaut, B. S. (2013). Gene body methylation is conserved between plant orthologs and is of evolutionary consequence. *Proceedings of the National Academy of Sciences of the United States of America*, 110(5), 1797–1802. <https://doi.org/10.1073/pnas.1215380110>
- Takuno, S., Ran, J.-H., & Gaut, B. S. (2016). Evolutionary patterns of genic DNA methylation vary across land plants. *Nature Plants*, 2(2), 15222. <https://doi.org/10.1038/nplants.2015.222>
- Trucchi, E., Mazzarella, A. B., Gilfillan, G. D., Lorenzo, M. T., Schönswetter, P., & Paun, O. (2016). BsRADseq: Screening DNA methylation in natural populations of non-model species. *Molecular Ecology*, 25(8), 1697–1713. <https://doi.org/10.1111/mec.13550>
- van Oppen, M. J. H., Oliver, J. K., Putnam, H. M., & Gates, R. D. (2015). Building coral reef resilience through assisted evolution. *Proceedings of the National Academy of Sciences*, 112(8), 1–7. <https://doi.org/10.1073/pnas.1422301112>
- Vidalis, A., Živković, D., Wardenaar, R., Roquis, D., Tellier, A., & Johannes, F. (2016). Methylome evolution in plants. *Genome Biology*, 17(1), 1–14. <https://doi.org/10.1186/s13059-016-1127-5>
- Wang, S., Lv, J., Zhang, L., Dou, J., Sun, Y., Li, X., Fu, X., Dou, H., Mao, J., Hu, X., & Bao, Z. (2015). MethylRAD: A simple and scalable method for genome-wide DNA methylation profiling using methylation-dependent restriction enzymes. *Open Biology*, 5(11), 150130. <https://doi.org/10.1098/rsob.150130>
- Wong, J. M., Johnson, K. M., Kelly, M. W., & Hofmann, G. E. (2018). Transcriptomics reveal transgenerational effects in purple sea urchin embryos: Adult acclimation to upwelling conditions alters the response of their progeny to differential pCO<sub>2</sub> levels. *Molecular Ecology*, 27(5), 1120–1137. <https://doi.org/10.1111/mec.14503>

- Wright, R. M., Aglyamova, G. V., Meyer, E., & Matz, M. V. (2015). Gene expression associated with white syndromes in a reef building coral. *Acropora Hyacinthus*. *BMC Genomics*, 16(1), 371. <https://doi.org/10.1186/s12864-015-1540-2>
- Zemach, A., & Zilberman, D. (2010). Evolution of Eukaryotic DNA Methylation and the Pursuit of Safer Sex. *Current Biology*, 20(17), R780–R785. <https://doi.org/10.1016/j.cub.2010.07.007>
- Zhang, X., Wu, M., Xiao, H., Lee, M. T., Levin, L., Leung, Y. K., & Ho, S. M. (2010). Methylation of a single intronic CpG mediates expression silencing of the PMP24 gene in prostate cancer. *Prostate*, 70(7), 765–776. <https://doi.org/10.1002/pros.21109>
- Zilberman, D. (2017). An evolutionary case for functional gene body methylation in plants and animals. *Genome Biology*, 18(1), 87. <https://doi.org/10.1186/s13059-017-1230-2>

## SUPPORTING INFORMATION

Additional supporting information may be found online in the Supporting Information section.

**How to cite this article:** Dixon G, Matz M. Benchmarking DNA methylation assays in a reef-building coral. *Mol Ecol Resour*. 2021;21:464–477. <https://doi.org/10.1111/1755-0998.13282>